

Decaying light particles in the SHiP experiment. III. Signal rate estimates for scalar and pseudoscalar goldstinos

K. O. Astapov^{1,2,*} and D. S. Gorbunov^{1,3,†}

¹*Institute for Nuclear Research of the Russian Academy of Sciences, Moscow 117312, Russia*

²*Physics Department, Moscow State University, Vorobievsky Gory, Moscow 119991, Russia*

³*Moscow Institute of Physics and Technology, Dolgoprudny 141700, Russia*

For supersymmetric extensions of the Standard Model with light goldstinos—scalar and pseudoscalar superpartners of goldstinos—we estimate the signal rate anticipated at the recently proposed fixed target experiment SHiP utilizing a CERN Super Proton Synchrotron beam of 400 GeV protons. We also place new limits on the model parameters from a similar analysis of the published results of the CHARM experiment.

I. INTRODUCTION

Low energy supersymmetry (SUSY) is perhaps the most developed extension of the Standard Model (SM) of particle physics [1, 2]. While, inherent in supersymmetry, a technically natural solution to the gauge hierarchy problem implies the SM superpartners are at or below the TeV energy scale, other and much lighter new particles can exist as well. In particular, if supersymmetry is spontaneously broken at not very high energy scales (see models with gauge mediation of supersymmetry breaking [3, 4] as an example), the particles from the SUSY breaking sector may show up at quite low energies. Their effective couplings to the SM particles are anticipated to be rather weak; therefore a high intensity beam is required to test the model via production of the new particles. The CERN Super Proton Synchrotron (SPS) provides us with a high intensity beam of 400 GeV protons, and the recently proposed beam-dump Search for Hidden Particles (SHiP) experiment [5] (see also Refs. [6, 7]) can perform the task (see Ref. [8] for a comprehensive discussion of the SHiP physics case).

The purpose of this paper is to estimate the signal rate expected at the SHiP experiment in supersymmetric models with sufficiently light particles of the *Goldstino supermultiplet*. The latter contains *Goldstino* (the Nambu–Goldstone field, fermion) and its superpartners, *scalar and pseudoscalar sgoldstinos*. While goldstinos are R odd, sgoldstinos are R even and hence can be singly produced in scatterings of the SM particles and can subsequently decay into the SM particles. Of particular interest are the sgoldstino decays into two electrically charged SM particles. These decays yield the signature well recognizable at SHiP [5]: two charged tracks from a single vertex supplemented with a peak in the invariant mass of outgoing particles. Sgoldstino couplings to the SM fields are inversely proportional to the parameter of the order of the squared scale of SUSY breaking in the whole model. This unique feature of the Goldstino supermultiplet allows us to probe the SUSY breaking scale

by hunting for the light goldstinos. A preliminary estimate of the sgoldstino signal for a particular production mechanism and decay channel can be found in Ref. [8]. Here we significantly extend that study by considering both scalar and pseudoscalar sgoldstinos and by investigating both flavor-conserving and flavor-violating sgoldstino couplings to the SM fermions, which cover various sgoldstino production mechanisms and decay modes.

The paper is organized as follows. Section II contains the sgoldstino effective Lagrangian. Section III and IV are devoted to SHiP phenomenology of scalar and pseudoscalar sgoldstinos, respectively. Here we discuss direct (Secs. III A and IV A) and indirect (Secs. III B and IV B) production mechanisms for flavor conserving and flavor violating sgoldstino coupling patterns. We consider various decay channels of scalar (Sec. III C) and pseudoscalar (Sec. IV C) sgoldstinos. We present our results (Secs. III D, III D, IV B and IV C) as estimates of the SHiP sensitivity to the SUSY breaking scale in particular supersymmetric variants of the SM. In Secs. III and IV we also put new limits on the model parameters by extending our analysis to the case of the CHARM experiment. We conclude in Sec. V by summarizing the results obtained.

II. SGOLDSTINO LAGRANGIAN

If supersymmetry exists, it is spontaneously broken in order to be phenomenologically viable [1]. The breaking happens when a hidden sector dynamics gives a nonzero vacuum expectation value F to an auxiliary component of a superfield. The dimension of this parameter is mass squared, and \sqrt{F} is of order of the SUSY breaking scale. The fermion component of this superfield, Goldstino \tilde{G} , becomes a longitudinal component of the gravitino as a result of the super-Higgs mechanism making the gravitino massive (for details see Ref. [9]). Goldstino superpartners, scalar S and pseudoscalar P sgoldstinos gain masses $m_{S,P}$ due to higher order corrections from the Kähler potential. The masses are largely model dependent and we merely keep them as free parameters in the (sub-)GeV range for this study.

Interaction of the Goldstino supermultiplet with other

* astapov@ms2.inr.ac.ru

† gorby@ms2.inr.ac.ru

fields is suppressed by the parameter F [9]. To the leading order in $1/F$, sgoldstino coupling to SM gauge fields [photons $F_{\mu\nu}$, gluons $G_{\mu\nu}^a$, where the index $a = 1, \dots, 8$ runs over $SU(3)$ color group generators] and matter fields

(leptons f_L , up and down quarks f_U and f_D) at the mass scale above Λ_{QCD} but below electroweak symmetry breaking reads [10, 11]

$$\begin{aligned} \mathcal{L}_{eff} = & -\frac{1}{2\sqrt{2}F} \left(m_S^2 S \bar{G} \tilde{G} + i m_P^2 P \bar{G} \gamma_5 \tilde{G} \right) - \frac{1}{2\sqrt{2}} \frac{M_{\gamma\gamma}}{F} S F^{\mu\nu} F_{\mu\nu} + \frac{1}{4\sqrt{2}} \frac{M_{\gamma\gamma}}{F} P \epsilon^{\mu\nu\rho\sigma} F_{\mu\nu} F_{\rho\sigma} - \frac{1}{2\sqrt{2}} \frac{M_3}{F} S G^{\mu\nu a} G_{\mu\nu}^a \\ & + \frac{1}{4\sqrt{2}} \frac{M_3}{F} P \epsilon^{\mu\nu\rho\sigma} G_{\mu\nu}^a G_{\rho\sigma}^a - \frac{\tilde{m}_{D_{ij}}^{LR 2}}{\sqrt{2}F} S \bar{f}_{D_i} f_{D_j} - i \frac{\tilde{m}_{D_{ij}}^{LR 2}}{\sqrt{2}F} P \bar{f}_{D_i} \gamma_5 f_{D_j} - \frac{\tilde{m}_{U_{ij}}^{LR 2}}{\sqrt{2}F} S \bar{f}_{U_i} f_{U_j} - i \frac{\tilde{m}_{U_{ij}}^{LR 2}}{\sqrt{2}F} P \bar{f}_{U_i} \gamma_5 f_{U_j} \\ & - \frac{\tilde{m}_{L_{ij}}^{LR 2}}{\sqrt{2}F} S \bar{f}_{L_i} f_{L_j} - i \frac{\tilde{m}_{L_{ij}}^{LR 2}}{\sqrt{2}F} P \bar{f}_{L_i} \gamma_5 f_{L_j}. \quad (1) \end{aligned}$$

Here M_3 is the gluino mass, $M_{\gamma\gamma} = M_1 \sin^2 \theta_W + M_2 \cos^2 \theta_W$ with M_1 and M_2 being $U(1)_Y$ - and $SU(2)_W$ -gaugino masses and θ_W the weak mixing angle, and $\tilde{m}_{U_{ij}}^{LR 2}$ and $\tilde{m}_{D_{ij}}^{LR 2}$ are left-right up- and down- squark soft mass terms. Lagrangian (1) includes only single-sgoldstino terms; considered in Refs. [10, 12–14], two-sgoldstino terms are suppressed by $1/F^2$ and are less promising for testing at the SHiP experiment. In the interesting range of F here, the gravitino is very light and can be safely replaced by its Goldstino component \tilde{G} , entering (1), whenever sgoldstino phenomenology at the beam-dump experiment is considered. Hence, sgoldstino couplings to the SM fields are proportional to the soft supersymmetry breaking parameters of the minimal supersymmetric extension of the SM (MSSM).

Sgoldstinos also mix with neutral Higgs bosons as described in Refs. [15–17]: the scalar sgoldstino S mixes with neutral light h and heavy H Higgs bosons, while pseudoscalar P mixes with axial Higgs A . In what follows we only account for the first mixing, since the other two do not change the sgoldstino phenomenology at SHiP for the set of models we investigate. Mixing of the sgoldstino and lightest MSSM Higgs boson (SM-like Higgs) h can be written as [17]

$$\mathcal{L}_{mixing} = \frac{X}{F} S h, \quad (2)$$

where the mixing parameter X is related to the Higgsino mixing mass parameter μ , the Higgs vacuum expectation value (vev) $v = 174$ GeV, the parameter $\tan \beta$ describing the Higgs vev ratio, and $SU(2)_W$ and $U(1)_Y$ gauge coupling constants g_2 and g_1 as follows

$$X = 2\mu^3 v \sin 2\beta + \frac{1}{2} v^3 (g_1^2 M_1 + g_2^2 M_2) \cos^2 2\beta. \quad (3)$$

We consider sgoldstino S to be much lighter than the SM-like Higgs boson of mass $m_h \approx 125$ GeV. Therefore, at low energies the above mixing ensures the Higgs-like couplings between the scalar sgoldstino and all the other SM fields. All the couplings are suppressed by the mixing

angle

$$\theta = -\frac{X}{F m_h^2}. \quad (4)$$

To illustrate the sensitivity of the SHiP experiment to sgoldstino couplings, in the next sections we present numerical results for the set of values of MSSM parameters (the benchmark point in the MSSM parameter space) shown in Table I. It is an arbitrary choice, except we

M_1 , GeV	M_2 , GeV	M_3 , GeV	μ , GeV	$\tan \beta$
100	250	1500	1000	6
m_A , GeV	A_l , GeV	m_l , GeV	A_Q , GeV	m_Q , GeV
1000	2800	1000	2800	1000

TABLE I. MSSM benchmark point.

suppose that all the model parameters take experimentally allowed values and the lightest Higgs boson mass is 125 GeV. Trilinear soft supersymmetry breaking parameters $A_{l,Q}$ are defined by the relations $\tilde{m}_{D_{ii}}^{LR 2} \equiv m_{D_i} A_Q$, $\tilde{m}_{U_{ii}}^{LR 2} \equiv m_{U_i} A_Q$, $\tilde{m}_{L_{ii}}^{LR 2} \equiv m_{L_i} A_l$, where we use SM fermion masses m_{D_i, U_i, L_i} ; m_A, m_Q, m_l are CP -odd Higgs boson, squark and slepton masses, correspondingly.

III. SCALAR SGOLDSTINO

In this section we consider two different production mechanisms of the scalar sgoldstino relevant for the SHiP setup. The first one is the direct production via hard gluon fusion in proton scatterings off the target material. The second one is the production in decays of mesons emerging due to the proton scattering.

A. Gluon fusion

If the sgoldstino is much heavier than the QCD energy scale of 100 MeV, it can be produced directly via gluon

fusion. The relevant parts of the sgoldstino interaction Lagrangians (1), (2), (4) read

$$\mathcal{L}_{Sgg} = \left(\theta g_{hgg}^{one-loop}(m_S) - \frac{\alpha_s(m_S)\beta(\alpha_s(M_3))}{\beta(\alpha_s(m_S))\alpha_s(M_3)} \frac{M_3}{2\sqrt{2}F} \right) \times SG^{\mu\nu a} G_{\mu\nu}^a, \quad (5)$$

where the first term, associated with Higgs-sgoldstino mixing (2), is proportional to the Higgs effective coupling to gluons (appearing at one-loop level via virtual quark exchanges) [18],

$$g_{hgg}^{one-loop} = \frac{3}{4} \frac{\alpha_s(m_S)}{6\sqrt{2}\pi v} \left(\mathcal{A}_{1/2}(\tau_t) + \mathcal{A}_{1/2}(\tau_b) + \mathcal{A}_{1/2}(\tau_c) + \mathcal{A}_{1/2}(\tau_s) \right). \quad (6)$$

Here $\tau_i = \frac{4m_i^2}{m_h^2}$, and loop form factors read

$$\mathcal{A}_{1/2} = 2\tau(1 + (1 - \tau)f(\tau)) \quad (7)$$

with

$$f(\tau) = \begin{cases} \arcsin^2(1/\sqrt{\tau}), & \tau \geq 1, \\ -\frac{1}{4} \log \frac{1+\sqrt{1-\tau}}{1-\sqrt{1-\tau}}, & \tau < 1. \end{cases} \quad (8)$$

The factor in front of the second term in Eq. (5) accounts for the renormalization group evolution with $\beta(\alpha_s)$ being the QCD β function. Note that both terms in Eq. (5) are inversely proportional to supersymmetry breaking parameter F .

To obtain a reliable estimate of the direct scalar sgoldstino cross section $\sigma_{pp \rightarrow S}$, we properly rescale the results of Ref. [19], where a coupling similar to Eq. (5) is responsible for the light inflaton production at the fixed target experiment with a 400 GeV proton beam. For the MSSM parameters from Table I we find the following numerical approximation to the cross section as a function of the sgoldstino mass and supersymmetry breaking parameter,

$$\begin{aligned} \log_{10} \left(\frac{\sigma_{pp \rightarrow S}}{\sigma_{pp, \text{total}}} \right) &= -15.8666 - 0.93934 \times \left(\frac{m_S}{1 \text{ GeV}} \right) \\ &+ 0.02025 \times \left(\frac{m_S}{1 \text{ GeV}} \right)^2 + 0.00052 \times \left(\frac{m_S}{1 \text{ GeV}} \right)^3 \\ &- 4 \log_{10} \left(\frac{\sqrt{F}}{100 \text{ TeV}} \right), \end{aligned} \quad (9)$$

where $\sigma_{pp, \text{total}}$ is the total pp cross section for the 400 GeV proton beam. This approximation is illustrated in Fig. 1 for two reference values of \sqrt{F} . Given the number of protons on target expected at SHiP, about 2×10^{20} [5], one concludes from Fig. 1 that the direct production can provide us with sgoldstinos only in the models with a supersymmetry breaking scale below 1000 TeV, if the MSSM superpartner scale is in the TeV range.

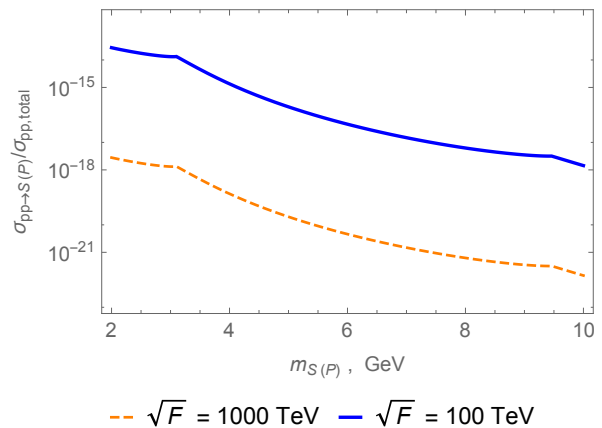


FIG. 1. Cross sections of scalar and pseudoscalar sgoldstino production in gluon fusion as functions of sgoldstino mass. No difference between scalar and pseudoscalar cases is expected.

B. B meson decays

Scalar sgoldstinos of masses in the GeV range are dominantly produced by decays of heavy mesons appearing by proton scattering off target. In the context of the SHiP experiment the main source of sgoldstinos is decays of B mesons. Decays of charmed mesons are suppressed as compared to beauty meson decays due to the smallness of the CKM (Cabibbo – Kobayashi – Maskawa) matrix element in the corresponding amplitude. The process is described by the triangle diagram with a t quark and W bosons running in the loop. The sgoldstino is emitted by the virtual t quark through sgoldstino-top-top coupling (1) and sgoldstino-Higgs mixing (2) (the latter dominates for the values shown in Table I). Adopting the same logic as used in [19] for the light inflaton, we calculate the branching ratio of B -meson decay into S ,

$$\begin{aligned} \text{Br}(B \rightarrow X_s S) &= \\ &= 0.3 \times \left(\frac{m_t}{m_W} \right)^4 \times \left(1 - \frac{m_S^2}{m_b^2} \right)^2 \times (A_Q v + F\theta)^2 \times \\ &\quad \times \left(\frac{100 \text{ TeV}}{\sqrt{F}} \right)^4, \end{aligned} \quad (10)$$

where X_s stands for the strange meson channel mostly saturated by a sum of pseudoscalar and vector kaons; m_b, m_t and m_W stand for b, t quarks and W^\pm boson masses, correspondingly. The scalar sgoldstino production cross section is then a product of the branching ratio above and the beauty cross section evaluated at the SHiP energy scale as $1.6 \times 10^{-7} \times \sigma_{pp, \text{total}}$ [5].

In Fig. 2 we compare the sgoldstino production cross sections provided by the direct and the indirect mechanisms for the same value of the supersymmetry breaking parameter, $\sqrt{F} = 100 \text{ TeV}$. One can observe from Eqs. (9) and (10) that both cross sections scale as \propto

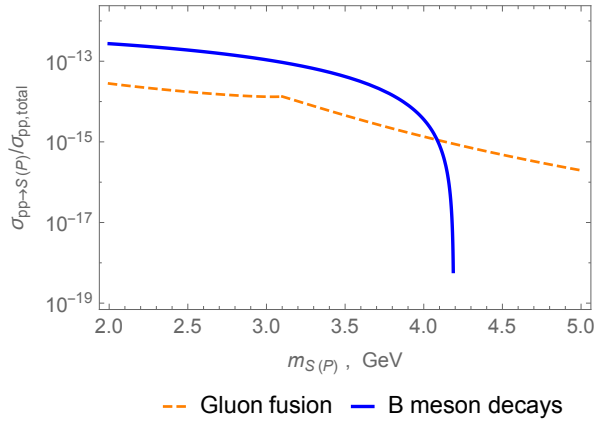


FIG. 2. Cross sections of scalar sgoldstino production in gluon fusion and in B -meson decays for the model with $\sqrt{F} = 100$ TeV. The same results are valid for the pseudoscalar sgoldstino production.

$1/F^2$. Thus, we conclude from the plot in Fig.2 that the meson channel dominates sgoldstino production when the kinematics allows. In what follows we concentrate on this case and comment on prospects of searches for the heavier sgoldstinos, $M_{S(P)} \gtrsim 4$ GeV, (available only via the direct production) in due course.

C. Sgoldstino decay pattern

The sgoldstino is R even and can decay into pairs of SM particles, if it is kinematically allowed. For the sgoldstino of the (sub-)GeV mass-range, the main decay channels are $\gamma\gamma$, e^+e^- , $\mu^+\mu^-$, $\pi^0\pi^0$, $\pi^+\pi^-$, K^+K^- , $K^0\bar{K}^0$ (see Ref. [10] for details).

The rate of sgoldstino decay into photons is described by the following expression:

$$\Gamma(S \rightarrow \gamma\gamma) = \left(\frac{\alpha(m_S)\beta(\alpha(M_{\gamma\gamma}))}{\beta(\alpha(m_S))\alpha(M_{\gamma\gamma})} \right)^2 \frac{m_{S(P)}^3 M_{\gamma\gamma}^2}{32\pi F^2}. \quad (11)$$

Here the dimensionless multiplicative factor accounts for the renormalization group evolution of the photonic operator at different mass scales. For sgoldstino decays into leptons one finds

$$\Gamma(S \rightarrow l^+l^-) = \frac{m_S^3 A_l^2 m_l^2}{16\pi F^2 m_S^2} \left(1 - \frac{4m_l^2}{m_S^2} \right)^{3/2}. \quad (12)$$

If the scalar is light ($m_S < 1.2$ GeV) then its decay into light mesons is described by the effective interaction involving the gluonic operator at a low energy scale, as explained in Ref. [10]. It yields the rates of sgoldstino

decays into mesons, e.g.,

$$\Gamma(S \rightarrow \pi^0\pi^0) = \frac{\alpha_s^2(M_3)}{\beta^2(\alpha_s(M_3))} \frac{\pi m_S m_S^2 M_3^2}{4 F^2} \left(1 - \frac{\beta(\alpha_s(M_3))}{\alpha_s(M_3)} \frac{9}{4\pi} \frac{B_0}{m_S} \frac{m_u + m_d}{m_S} \frac{A_Q}{M_3} \right)^2 \sqrt{1 - \frac{4m_{\pi^0}^2}{m_S^2}}, \quad (13)$$

where $\beta(\alpha_s)$ is the QCD beta function, $\alpha_s(M_3)$ is the strong coupling constant evaluated at the scale of M_3 , and the parameter B_0 can be expressed via masses of kaons and quarks as $B_0 = M_K^2/(m_d + m_s)$.

It turns out that for our benchmark point (see Table I) the contribution to Eq. (13) from the gluonic operator dominates over the quark operator contribution, so we have

$$\Gamma(S \rightarrow \pi^0\pi^0) \approx \frac{\alpha_s^2(M_3)}{\beta^2(\alpha_s(M_3))} \frac{\pi m_S^3 M_3^2}{4F^2} \sqrt{1 - \frac{4m_{\pi^0}^2}{m_S^2}}, \quad (14)$$

$$\Gamma(S \rightarrow \pi^+\pi^-) = 2\Gamma(S \rightarrow \pi^0\pi^0), \quad (15)$$

and analogously for kaons:

$$\Gamma(S \rightarrow K^0\bar{K}^0) \approx \frac{4\alpha_s^2(M_3)}{\beta^2(\alpha_s(M_3))} \frac{\pi m_S^3 M_3^2}{4F^2} \sqrt{1 - \frac{4m_K^2}{m_S^2}}, \quad (16)$$

$$\Gamma(S \rightarrow K^+K^-) = \Gamma(S \rightarrow K^0\bar{K}^0). \quad (17)$$

For the sgoldstino masses well above the QCD mass scale ($m_S \gg 1$ GeV) the decay into hadrons can be described as decay into a gluon pair, which then hadronizes. Its rate reads

$$\Gamma(S \rightarrow gg) = \left(\frac{\alpha_s(m_S)\beta(\alpha_s(M_3))}{\beta(\alpha_s(m_S))\alpha_s(M_3)} \right)^2 \frac{m_S^3 M_3^2}{4\pi F^2}. \quad (18)$$

The multiplicative factor is added above to correct for the renormalization group evolution of the gluonic operator with mass scale.

Between these mass ranges, where $m_s \approx 1.2 - 4$ GeV, neither description method is reliable where some heavy mesons, as well as multimeson final states, enter the game. However, comparing contributions for relevant hadronic modes calculated within these two approaches, we observe that deviations do not exceed an order of magnitude. Thus, we conclude that order-of-magnitude estimates of the sgoldstino lifetime for the mass interval 1.2 – 4 GeV can be obtained by some extrapolation of the chiral theory approach.

The branching ratios of the scalar sgoldstino decays for the values of MSSM soft parameters chosen in Table I are shown in Fig. 3. Hadronic channels, $\pi\pi$, KK , naturally dominate (if kinematically allowed), while $\gamma\gamma$ and $\mu^+\mu^-$ give small but noticeable contributions. Decay rates (11)–(17) ensure that each branching ratio scales

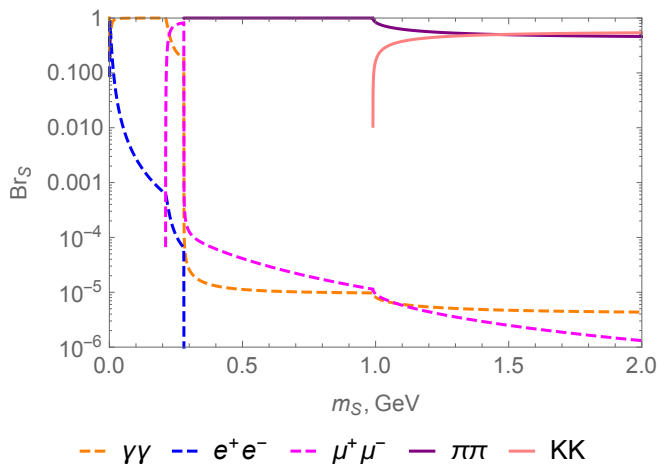


FIG. 3. Branching ratios of a scalar sgoldstino.

as the square of the corresponding soft supersymmetry breaking parameter, e.g., $\text{Br}(S \rightarrow \mu^+\mu^-) \propto A_t^2$.

Heavier sgoldstinos decay mostly into gluons. The invisible decay mode $S \rightarrow \tilde{G}\tilde{G}$ is always negligible because the corresponding coupling in Eq. (1) is proportional to the sgoldstino mass squared rather than the MSSM soft terms. The sgoldstino lifetime for a set of values of F is presented in Fig. 4. To reach the main detector of the

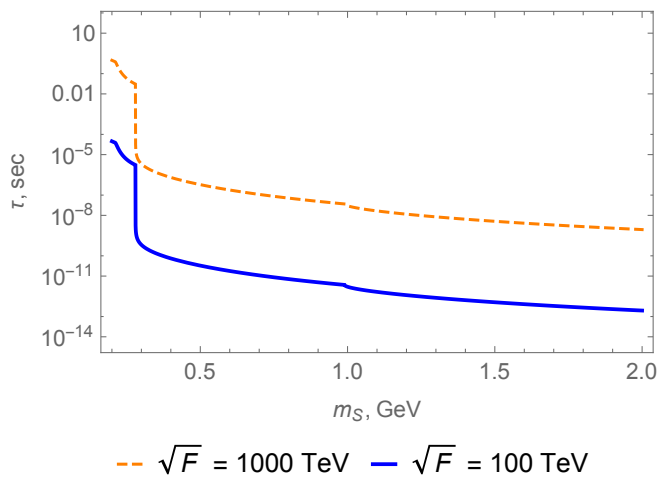


FIG. 4. Lifetime of a scalar sgoldstino as a function of its mass.

SHiP experiment, the sgoldstino has to cover a distance of about 100 meters [5]. The results in Fig. 4 suggest that SHiP can be sensitive mostly to the models with supersymmetry breaking scale of about 100 TeV and higher. The lifetime scales as $\tau \propto F^2$ and as $\tau \propto 1/M_3^2$ since the hadron channel dominates.

D. Sgoldstino signal event rate at SHiP

Now we collect all the ingredients required to achieve the main goal of this article, the estimate of the number of sgoldstino decay events inside the fiducial volume of the SHiP experiment. The SHiP construction is outlined in Ref. [5]. The 400 GeV proton beam fueled by the SPS hits the target and produces bunches of mesons, which can decay into new particles (sgoldstinos in the case at hand). The latter can also appear directly from the proton-proton collisions (through gluon fusion). The detector is placed at a distance of $l_{sh} = 63.8$ m from the target. The vacuum vessel length is about $l_{det} = 60$ m. It forms a cylinder along the beam axis with an elliptical base of 5×10 m. The trajectories of electrically charged particles emerging from the new particle decays can be traced in the detector volume and their energies and types can be determined by the registration system utilizing devices arranged at the far end of the detector.

The differential production cross section of sgoldstinos, originated from the B meson decays, has the following form,

$$\frac{d^3\sigma_{pp \rightarrow S(P)}}{dpd\theta_p d\phi_p} = \int d^3\vec{k} f(\vec{p}, \vec{k}) \frac{d^3\sigma_B}{dkd\theta_k d\phi_k}, \quad (19)$$

where $f(\vec{p}, \vec{k})$ is the sgoldstino momentum distribution normalized to the branching ratio (10) and $\frac{d^3\sigma_B}{dkd\theta_k d\phi_k}$ is the differential production cross section of B -mesons in proton-proton collisions, which is evaluated along the lines of Ref. [20]. In the integral (19) the total values of the 3-momenta and escaping angle of the outgoing particles are specifically constrained to ensure that the sgoldstino trajectory crosses the rear end of the SHiP detector, which defines the fiducial volume.

With the above approximations we estimate the number of signal events as

$$N_{\text{signal}} = \frac{N_{\text{POT}}}{\sigma_{pp, \text{total}}} \int w_{det} \frac{d\sigma_{pp \rightarrow S(P)}}{dpd\theta_p d\phi_p} d^3\vec{p}, \quad (20)$$

where the expected number of protons on the target is $N_{\text{POT}} = 2 \times 10^{20}$ [8] and w_{det} denotes the probability for the sgoldstino to decay inside the fiducial volume of the detector,

$$w_{det}(E_{S(P)}, m_{S(P)}, \sqrt{F}) = \exp(-l_{sh}/\gamma c\tau_{S(P)}) \times [1 - \exp(-l_{det}/\gamma(E_{S(P)})c\tau_{S(P)})], \quad (21)$$

with the sgoldstino gamma factor $\gamma(E_{S(P)}) = E_{S(P)}/m_{S(P)}$.

In Fig. 5 we indicate the region in the model parameter space $(m_{S(P)}, 1/\sqrt{F})$, where the number of sgoldstino decays inside the SHiP fiducial volume exceeds 3, $N_{\text{signal}} > 3$. That is, if no events were observed (the background for the two-body decays into charged SM particles is zero [5]) the region is excluded at the confidence level of 95%, in accordance with the Poisson statistics.

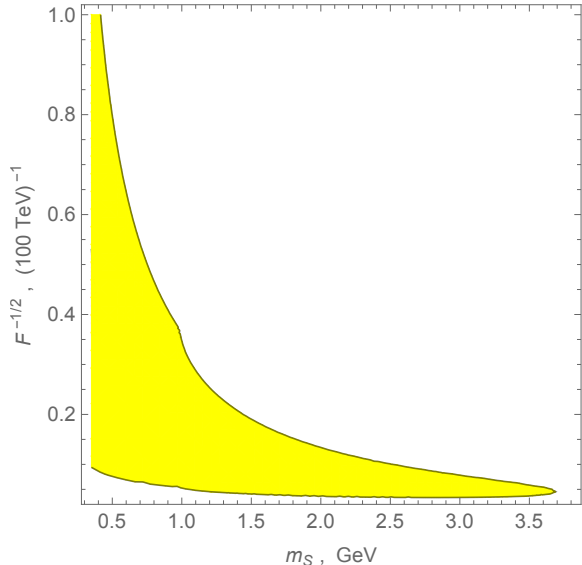


FIG. 5. The shaded region will be probed at the SHiP experiment.

The upper boundary in Fig. 5 is the region where the sgoldstino coupling constants $\propto 1/F$ are large enough to initiate very fast decay of the sgoldstino before it reaches the detector. The lower boundary in Fig. 5 is the region where the couplings are so small that sgoldstinos escape from the detector without decay. The number of signal events here scales with the model parameters as $N_{\text{signal}} \propto M_3^2 \mu^6 / F^4$. The region in Fig. 5 of the heaviest sgoldstino reachable at SHiP, $m_S \approx 3.6$ GeV, is the meeting point of the lower and the upper boundaries. Here, the sgoldstino decay length is about 100 m, which is the scale of both the SHiP detector length and the distance from the target, $\gamma c\tau \sim l_{\text{det}} \sim l_{\text{sh}}$. In this case the number of signal events scales as $N_{\text{signal}} \propto \mu^6 / F^2$. The scalings of the signal events imply that models with a higher (as compared to that presented in Fig. 5) scale of supersymmetry breaking can be tested if MSSM parameters μ , M_3 are appropriately bigger (as compared to those presented in Table I).

Sgoldstinos of masses 3.6–4.2 GeV, which can be produced through B -meson decays (see Figs. 2 and 5), seem to be beyond the SHiP’s grip for our choice of MSSM parameters presented in Table I. However, the signal scaling with model parameters explained above suggests that sgoldstinos of masses above 3.6 GeV can be tested at SHiP in models with a higher scale of SM superpartners. Finally, from the results presented in Figs. 2 and 4 one can conclude that sgoldstinos of masses above 4 GeV, which can appear only via direct production, cannot be tested at SHiP. Both sgoldstino production and decay are governed by the same ratio M_3^2 / F^2 , and the sgoldstino lifetime $\tau \propto 1/m_S^3$ is too short for the reasonably high sgoldstino production. One needs much higher intensity of the proton beam at SPS to probe this region of model

parameter space.

E. Flavor violating

In supersymmetric models with nondiagonal sfermion left-right mass terms, $\tilde{m}_{D_{ij}}^{LR 2} \not\propto \delta_{ij}$, etc, sgoldstino couplings (1) violate flavor symmetry. These flavor-violating terms are additional sources of sgoldstino production in a beam-target experiment. To illustrate the point, here we consider flavor-violating decays of (produced by protons on target) B and D_s mesons into kaons and light scalar sgoldstinos. These processes are governed by the soft parameters $\tilde{m}_{D_{23}}^{LR 2}$ and $\tilde{m}_{U_{12}}^{LR 2}$. Observation of oscillations in the $B^0 - \bar{B}^0$ and $D^0 - \bar{D}^0$ systems and searches for very rare (within the SM) decays like $B \rightarrow \mu^+ \mu^-$ constrain [21, 22] possible flavor violation in the squark sector, which for our reference point given in Table I imposes the following upper limits on the off-diagonal entries,

$$\tilde{m}_{D_{23}}^{LR 2} < 0.02 \text{ TeV}^2, \quad \tilde{m}_{U_{12}}^{LR 2} < 0.016 \text{ TeV}^2. \quad (22)$$

The above flavor-violating interaction terms yield the decay rates

$$\begin{aligned} \Gamma(B \rightarrow KS) &= \\ &= F_{B \rightarrow K}^2 \left(\frac{m_B^2 - m_K^2}{m_b + m_u} \right)^2 \frac{\lambda_{B \rightarrow KS}}{16\pi^2 m_B^3} \frac{\tilde{m}_{D_{23}}^{LR 4}}{F^2} \end{aligned} \quad (23)$$

and

$$\begin{aligned} \Gamma(D_s \rightarrow KS) &= \\ &= F_{D_s \rightarrow K}^2 \left(\frac{m_{D_s}^2 - m_K^2}{m_c + m_u} \right)^2 \frac{\lambda_{D_s \rightarrow KS}}{16\pi^2 m_{D_s}^3} \frac{\tilde{m}_{U_{12}}^{LR 4}}{F^2}, \end{aligned} \quad (24)$$

where

$$\lambda_{B(D_s) \rightarrow KS} = \sqrt{(m_{B(D_s)}^2 - m_K^2 - m_S^2)^2 - 4m_{B(D_s)}^2 m_K^2},$$

and dimensionless form factors $F_{B \rightarrow K}$ and $F_{D_s \rightarrow K}$ are given in Ref. [23].

To illustrate the sensitivity of the SHiP experiment to the flavor-violating sgoldstino couplings, we take the soft parameters $\tilde{m}_{U_{12}}^{LR 2}$ and $\tilde{m}_{D_{23}}^{LR 2}$ to be equal to their upper bounds (22) and other MSSM parameters as in Table I. Then, treating the flavor-violating meson decays as the main sources of sgoldstinos and repeating the analysis of Sec. III D, we obtain the expected exclusion plots for the SHiP experiment (see Fig. 6). Similar to Fig. 5, the lower margins refer to the limit of tiny couplings of the sgoldstino to the SM fields. The numbers of sgoldstino decays here scale with the relevant model parameters as $N_{\text{signal}} \propto \tilde{m}_{D_{23}(U_{12})}^{LR 4} M_3^2 / F^4$.

Note that sgoldstinos can be directly searched for in the appropriate decay modes of the heavy mesons (for examples, see Refs. [10, 14, 27, 28]). In particular, the process $B \rightarrow K_s + S(P)$ with sgoldstinos subsequently

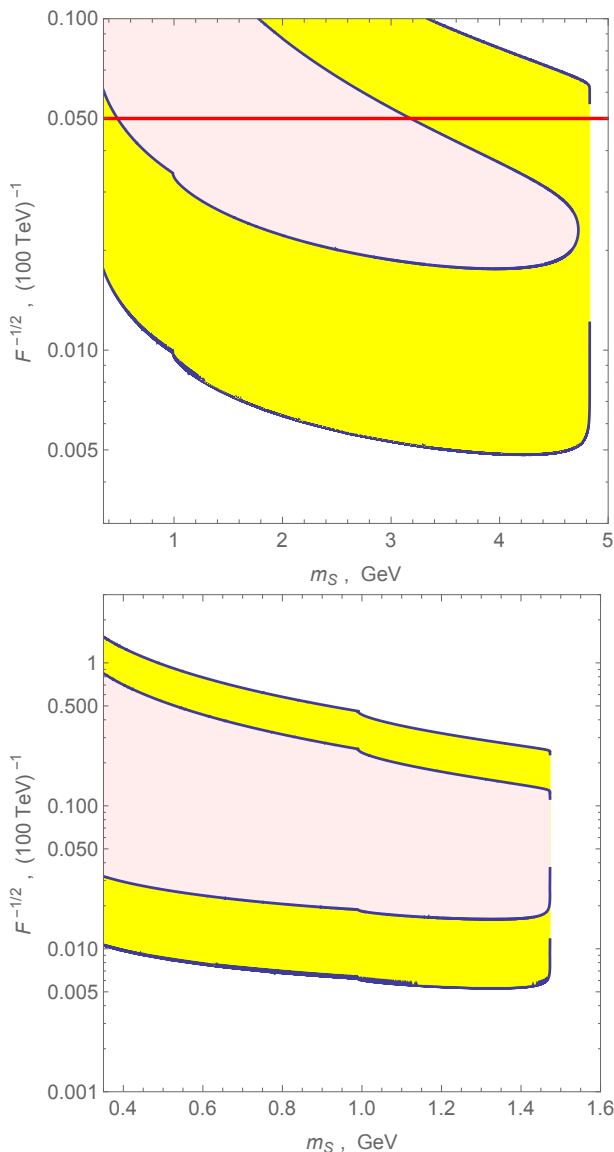


FIG. 6. Yellow shaded regions are expected to be excluded (95% C.L.) at the SHiP experiment, if the flavor-violating soft parameters $\tilde{m}_{D_{23}}^{LR}$ (top panel) and $\tilde{m}_{U_{12}}^{LR}$ (bottom panel) take their present upper limits for the benchmark point in Table I. The region above the solid horizontal line on the top panel is excluded due to the negative result in searches for the three-body decay $B \rightarrow K_s^0 \nu \bar{\nu}$ [24]. Light red shaded regions are excluded by our analysis of the results of the CHARM experiment [25, 26].

decaying outside the detector can mimic the process $B \rightarrow h^{(*)} + \text{missing}$, whose branching is presently constrained as [24]

$$\text{Br}(B \rightarrow K_s^0 \nu \bar{\nu}) < 9.7 \times 10^{-5}. \quad (25)$$

At the chosen value of $\tilde{m}_{D_{23}}^{LR}$ the sgoldstino's contribution (if any) must be smaller than this limit. A similar requirement exists for the twin process with charged mesons. Thus, the region above the horizontal line in

Fig. 6 (top panel) is excluded by the constraint (25). This upper limit on $F^{-1/2}$ scales as $\propto \text{Br}^{1/4}/\tilde{m}_{D_{23}}^{LR}$.

Comparing Fig. 6 with Fig. 5 one concludes that SHiP exhibits higher sensitivity to the supersymmetric models with flavor violation. We extend the performed analysis to the CHARM experiment, which operated on the same proton beam at CERN, but collected much lower statistics and was placed at a much larger distance from the target as compared to the SHiP. Nevertheless, we find that in the case of flavor-violating sgoldstino coupling, we can exclude a part of the model parameter space (see Fig. 6) given the negative results of searches at CHARM [25, 26].

IV. PSEUDOSCALAR SGOLDSTINO

If parity is (strongly) violated in the sfermion sector of the MSSM, sgoldstino couplings to the SM fermions violate it, too. Then, scalar and pseudoscalar sgoldstinos are very similar as regards the SHiP phenomenology. However, if sgoldstino couplings conserve parity (that takes place, e.g., in left-right extensions of the MSSM), the phenomenology of pseudoscalar and scalar sgoldstins is different in some aspects (see Refs. [10, 27] for details). In this section we investigate SHiP sensitivity to the pseudoscalar sgoldstino couplings.

A. Light pseudoscalar production

The pseudoscalar sgoldstino P can be directly produced via the gluon fusion with the same cross section as the scalar sgoldstino; hence, Fig. 1 is valid for both cases. However, its production through the meson decays is somewhat different from that of the scalar sgoldstino because of the absence of mixing with the light MSSM Higgs.¹

The light pseudoscalar can be produced in B -meson decays. The corresponding one-loop diagram is very similar to that in the case of the scalar sgoldstino discussed in Sec. III B, but only the sgoldstino-top-top pseudoscalar coupling (1) contributes. Given the pseudoscalar nature of P , for the two-body decay it is accompanied by the vector kaon K^* . The decay rate can be obtained by properly replacing the coupling constants in the result presented in Ref. [29] for the case of decay into the axion, where we assume charged the Higgs boson mass m_H to be approximately 1 TeV, which follows from the value of

¹ There is a mixing with CP -odd Higgs A^0 , which is negligibly small for our choice of the benchmark point in Table I.

m_A given in Table I,

$$\Gamma(B \rightarrow K^* P) = \frac{G_F^2 m_t^2 m_{U33}^{RL 4}}{2^{13} \pi^3} \cot^2 \beta (\hat{X}_1 + \cot^2 \beta \hat{X}_2)^2 \times \frac{A_0^2 \lambda_{B \rightarrow K^*}^3}{m_B^3}, \quad (26)$$

where

$$\lambda_{B \rightarrow K^*} = \sqrt{(m_B^2 - m_P^2 - m_{K^*}^2)^2 - 4m_P^2 m_{K^*}^2}, \quad (27)$$

and

$$\begin{aligned} \hat{X}_1 = & 2 + \frac{m_H^2}{m_H^2 - m_t^2} - \frac{3m_W^2}{m_t^2 - m_W^2} + \\ & + \frac{3m_W^4 (m_H^2 + m_W^2 - 2m_t^2)}{(m_H^2 - m_W^2)(m_t^2 - m_W^2)^2} \ln \frac{m_t^2}{m_W^2} + \\ & + \frac{m_H^2}{m_H^2 - m_t^2} \left(\frac{m_H^2}{m_H^2 - m_t^2} - \frac{6m_W^2}{m_H^2 - m_W^2} \right) \ln \frac{m_t^2}{m_H^2}, \quad (28) \end{aligned}$$

$$\hat{X}_2 = -\frac{2m_t^2}{m_H^2 - m_t^2} \left(1 + \frac{m_H^2}{m_H^2 - m_t^2} \ln \frac{m_t^2}{m_W^2} \right), \quad (29)$$

and the dimensionless form factor A_0 can be found in Ref. [30]. Though the formula for the decay rate somewhat differs from that in the case of the scalar, they give very close numerical results, so the production rates are almost the same, Figure 2 refers to both cases.

B. Decay

In contrast to the scalar S , the pseudoscalar sgoldstino P does not decay into a meson pair. However, it mixes with pseudoscalar mesons π and η , as explained in Ref. [10]. Since mesons exhibit four-meson coupling, the pseudoscalar sgoldstino can decay into three mesons through the virtual meson state, $P \rightarrow \pi^{0*}/\eta^* \rightarrow 3$ mesons.

Inherent in the chiral perturbation theory the four-meson interaction reads [31]

$$\mathcal{L}_{eff} = \frac{1}{12f_\pi^2} \text{Tr}(\Phi \overleftrightarrow{\partial} \Phi \Phi \overleftrightarrow{\partial} \Phi), \quad (30)$$

where

$$\Phi = \begin{pmatrix} \frac{1}{\sqrt{2}}\pi^0 + \frac{1}{\sqrt{6}}\eta & \pi^+ & K^+ \\ \pi^- & -\frac{1}{\sqrt{2}}\pi^0 + \frac{1}{\sqrt{6}}\eta & K^0 \\ K^- & \bar{K}^0 & -\frac{2}{\sqrt{6}}\eta \end{pmatrix}. \quad (31)$$

It induces 4-meson operators $\mathcal{O}_4^{\pi^0(\eta)}$ and \mathcal{O}_4^η responsible for the interesting transitions $\pi^{0*}/\eta^* \rightarrow 3$ mesons.

Matrix elements of the initial off-shell π^0 meson (with squared 4-momentum $m_{\pi^{0*}}^2$) and three on-shell mesons in the final state are as follows:

$$\langle \pi^{0*} | \mathcal{O}_4^{\pi^0} | \pi^0 \pi^0 \pi^0 \rangle = \frac{1}{6f^2} (5m_{\pi^{0*}}^2 - 3m_{\pi^0}^2), \quad (32)$$

$$\langle \pi^{0*} | \mathcal{O}_4^{\pi^0} | \pi^0 \eta \eta \rangle = \frac{2}{3f^2} (2m_{\pi^{0*}}^2 + m_{\pi^0}^2 - 2m_\eta^2), \quad (33)$$

$$\langle \pi^{0*} | \mathcal{O}_4^{\pi^0} | \pi^0 K K \rangle = \frac{2}{3f^2} (2m_{\pi^{0*}}^2 + m_{\pi^0}^2 - 2m_K^2), \quad (34)$$

$$\langle \pi^{0*} | \mathcal{O}_4^{\pi^0} | \pi^0 \pi^+ \pi^- \rangle = \frac{2}{3f^2} (2m_{\pi^{0*}}^2 + m_{\pi^0}^2 - 2m_{\pi^+}^2). \quad (35)$$

One obtains similar expressions for the initial virtual η meson.

Finally we find for the pseudoscalar decay rate into 3 mesons:

$$\begin{aligned} \Gamma(P \rightarrow \pi^{0*}/\eta^* \rightarrow 3 \text{ mesons}) = & \\ = & \frac{f_\pi^2 \pi^2 m_\pi^4 \epsilon^2}{4(m_P^2 - m_\pi^2)^2} \frac{M_3^2}{F^2} \Gamma(\pi^* \rightarrow 3 \text{ mesons}) + \\ & + \frac{f_\pi^2 \pi^2 m_\eta^4}{4(m_P^2 - m_\eta^2)^2} \frac{M_3^2}{F^2} \Gamma(\eta^* \rightarrow 3 \text{ mesons}), \quad (36) \end{aligned}$$

where 3-body decay widths $\Gamma(\pi^*(\eta^*) \rightarrow 3 \text{ mesons})$ are calculated using the matrix elements (32) – (35) (and similarly for the η meson) assuming that squared 4-momenta of the off-shell π^* and η^* equal m_P^2 ; we also make use of $\epsilon = (m_u - m_d)/(m_u + m_d)$.

Pseudoscalar sgoldstino decay rates into photons and leptons have the forms (11) and (12), respectively, with the obvious replacement $m_S \rightarrow m_P$.

The pseudoscalar sgoldstino lifetime and its relevant decay branching ratios are presented in Figs. 7 and 8,

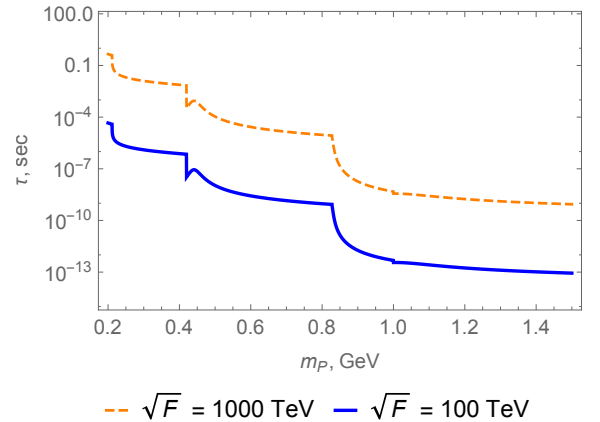


FIG. 7. Pseudoscalar sgoldstino lifetime for $\sqrt{F} = 100, 1000$ TeV (lines from bottom to top).

correspondingly. Hadronic channels, mainly 3π , ηKK , $\eta\pi\pi$ and 3η , dominate sgoldstino decay. Given its geometry, the SHiP experiment is sensitive to the supersymmetry breaking scales of about $\sqrt{F} \sim 100$ TeV and above.

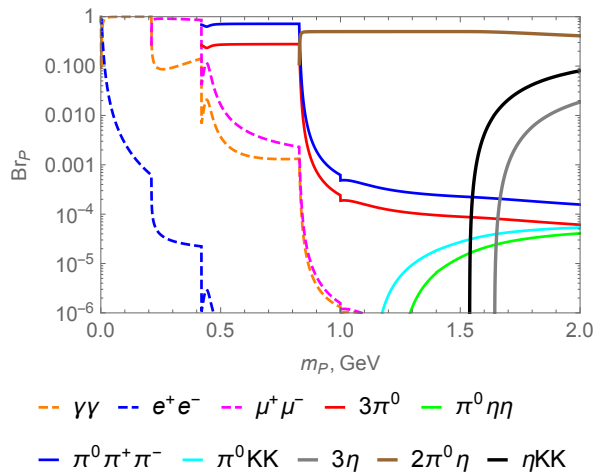


FIG. 8. Branchings ratios of the pseudoscalar sgoldstino.

Performing for the pseudoscalar case the same procedure as that adopted in Sec. III D for the scalar sgoldstino, we estimate the SHiP sensitivity to the pseudoscalar sgoldstino interaction. In Fig. 9 we present

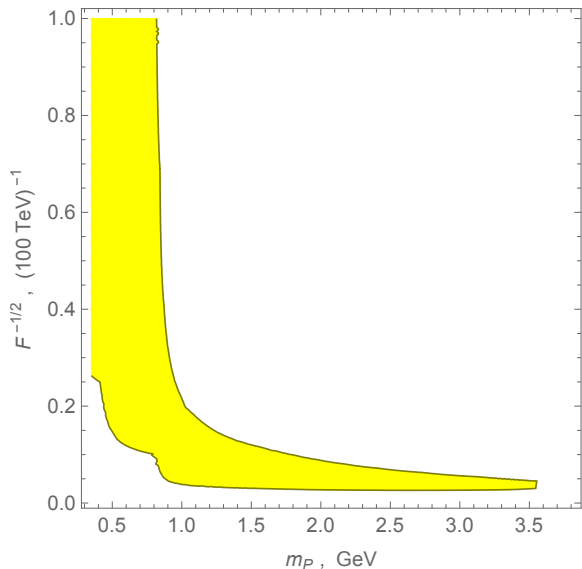


FIG. 9. The shaded region can be explored at the SHiP experiment.

the plot displaying the region in the parameter space $(F^{-1/2}, m_S)$ expected to be explored with the SHiP ex-

periment. One observes that in the case of the pseudoscalar sgoldstino the SHiP is sensitive to models with a lower SUSY breaking scale \sqrt{F} as compared to the scalar sgoldstino (cf. Figs. 5 and 9).

C. Flavor violation

The study of the flavor-violating pseudoscalar sgoldstino coupling is very similar to that of the scalar sgoldstino. These couplings induce two-body heavy meson decays into the pseudoscalar sgoldstino and a light vector meson (it replaces the pseudoscalar meson in the case of the scalar sgoldstino in the final state). For numerical estimates we adopt the same patterns of the flavor-violating couplings as used in the case of the scalar sgoldstino. The final estimates of the SHiP sensitivity to the pseudoscalar sgoldstino are presented in Fig. 10.

V. CONCLUSIONS

We have estimated sensitivity of the SHiP experiment to supersymmetric extensions of the SM where sgoldstinos are light. The proposed experiment will be able to probe the supersymmetry breaking scale \sqrt{F} up to 10^3 TeV for the model without flavor violation and up to 10^5 TeV for the model with flavor-violating parameters as large as the corresponding present experimental upper bounds. We have also compared the regions of the sgoldstino parameter space to be probed at the SHiP experiment with the regions that we have excluded from the analysis of the results of the CHARM experiment [25, 26]. The regions are outlined in Figs. 6 and 10: as one can see, the SHiP experiment will significantly extend our ability in testing supersymmetric models with light sgoldstinos.

In this paper we concentrate mostly on the models with sgoldstino masses in the range 0.4–4 GeV, where sgoldstino can be kinematically produced in decays of charm and beauty mesons. Lighter sgoldstinos can, in addition, be produced at the SHiP by strange meson decays. This possibility deserves a special study beyond the scope of this paper. Sgoldstinos can also be produced in decays of secondary mesons from the hadronic cascade developing in the target. These mesons are numerous, but less energetic. The proper account of this contribution requires numerical simulations of the hadronic cascade and a more accurate treatment of the SHiP geometry.

Acknowledgments We thank I. Timiryasov and S. Demidov for valuable discussions. The work was supported by the RSF Grant No. 14-22-00161.

[1] H. E. Haber and G. L. Kane, “The Search for Supersymmetry: Probing physics beyond the standard model,” *Phys. Rep.* **117**, 75 (1985).

[2] S. P. Martin, “A Supersymmetry primer, In *Kane, G.L. (ed.): Perspectives on supersymmetry II* 1-153 [hep-ph/9709356].

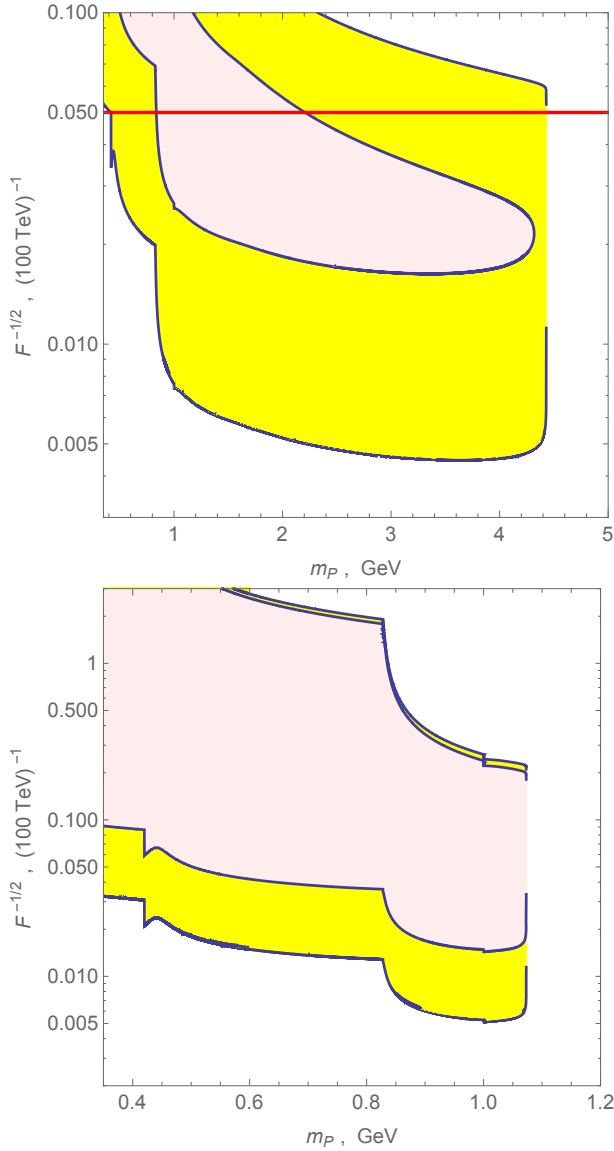


FIG. 10. Yellow shaded regions can be explored with the SHiP experiment in the case of nonzero soft parameters $\tilde{m}_{U_{12}}^{LR,2}$ (lower panel) and $\tilde{m}_{D_{23}}^{LR,2}$ (upper panel). The region above the solid horizontal line on the lower panel is excluded due to a negative result in searches for the three-body decay $B \rightarrow K_s^0 \nu \bar{\nu}$ [24]. Light red shaded regions are excluded by the analysis of the results of CHARM experiment [25, 26].

[3] G. F. Giudice and R. Rattazzi, “Theories with gauge mediated supersymmetry breaking,” *Phys. Rep.* **322** (1999) 419 [hep-ph/9801271],

[4] S. L. Dubovsky, D. S. Gorbunov and S. V. Troitsky, “Gauge mechanism of mediation of supersymmetry breaking,” *Phys. Usp.* **42** (1999) 623 [*Usp. Fiz. Nauk* **169** (1999) 705] [hep-ph/9905466].

[5] M. Anelli *et al.* [SHiP Collaboration], “A facility to Search for Hidden Particles (SHiP) at the CERN SPS,” arXiv:1504.04956 [physics.ins-det].

[6] S. N. Gninenko, D. S. Gorbunov and M. E. Shaposhnikov, “Search for GeV-scale sterile neutrinos responsible for

active neutrino oscillations and baryon asymmetry of the Universe,” *Adv. High Energy Phys.* **2012**, 718259 (2012) [arXiv:1301.5516 [hep-ph]].

[7] W. Bonivento *et al.*, “Proposal to Search for Heavy Neutral Leptons at the SPS,” arXiv:1310.1762 [hep-ex].

[8] S. Alekhin *et al.*, “A facility to Search for Hidden Particles at the CERN SPS: the SHiP physics case,” arXiv:1504.04855 [hep-ph].

[9] E. Cremmer, B. Julia, J. Scherk, P. van Nieuwenhuizen, S. Ferrara and L. Girardello, “Super-higgs effect in supergravity with general scalar interactions,” *Phys. Lett. B* **79** (1978) 231.

[10] D. S. Gorbunov, “Light sgoldstino: Precision measurements versus collider searches,” *Nucl. Phys. B* **602**, 213 (2001) [hep-ph/0007325].

[11] D. S. Gorbunov and A. V. Semenov, “CompHEP package with light gravitino and sgoldstinos, hep-ph/0111291.

[12] E. Perazzi, G. Ridolfi and F. Zwirner, “Signatures of massive sgoldstinos at e^+e^- colliders,” *Nucl. Phys. B* **574**, 3 (2000) [hep-ph/0001025].

[13] E. Perazzi, G. Ridolfi and F. Zwirner, “Signatures of massive sgoldstinos at hadron colliders,” *Nucl. Phys. B* **590**, 287 (2000) [hep-ph/0005076].

[14] S. V. Demidov and D. S. Gorbunov, “Flavor violating processes with sgoldstino pair production,” *Phys. Rev. D* **85**, 077701 (2012) [arXiv:1112.5230 [hep-ph]].

[15] E. Dudas, C. Petersson and P. Tziveloglou, “Low Scale Supersymmetry Breaking and its LHC Signatures,” *Nucl. Phys. B* **870**, 353 (2013) [arXiv:1211.5609 [hep-ph]].

[16] B. Bellazzini, C. Petersson and R. Torre, “Photophilic Higgs from sgoldstino mixing,” *Phys. Rev. D* **86**, 033016 (2012) [arXiv:1207.0803 [hep-ph]].

[17] K. O. Astapov and S. V. Demidov, “Sgoldstino-Higgs mixing in models with low-scale supersymmetry breaking,” *JHEP* **1501**, 136 (2015) [arXiv:1411.6222 [hep-ph]].

[18] J. R. Ellis, M. K. Gaillard, D. V. Nanopoulos, and C. T. Sachrajda, *Phys. Lett. B* **83**, 339 (1979).

[19] F. Bezrukov and D. Gorbunov, “Light inflaton Hunter’s Guide,” *JHEP* **1005** (2010) 010 [arXiv:0912.0390 [hep-ph]].

[20] D. Gorbunov and I. Timiryasov, “Decaying light particles in the SHiP experiment. II. Signal rate estimates for light neutralinos,” *Phys. Rev. D* **92**, no. 7, 075015 (2015) [arXiv:1508.01780 [hep-ph]].

[21] M. Ciuchini, E. Franco, D. Guadagnoli, V. Lubicz, M. Pierini, V. Porretti and L. Silvestrini, “ $D - \bar{D}$ mixing and new physics: General considerations and constraints on the MSSM,” *Phys. Lett. B* **655**, 162 (2007) [hep-ph/0703204].

[22] M. Arana-Catania, “The flavour of supersymmetry: Phenomenological implications of sfermion mixing,” arXiv:1312.4888 [hep-ph].

[23] T. Palmer and J. O. Eeg, “Form factors for semileptonic D decays,” *Phys. Rev. D* **89**, no. 3, 034013 (2014) [arXiv:1306.0365 [hep-ph]].

[24] O. Lutz *et al.* [Belle Collaboration], “Search for $B \rightarrow h^{(*)} \nu \bar{\nu}$ with the full Belle $\Upsilon(4S)$ data sample,” *Phys. Rev. D* **87**, no. 11, 111103 (2013) [arXiv:1303.3719 [hep-ex]].

[25] F. Bergsma *et al.* [CHARM Collaboration], “A Search for Decays of Heavy Neutrinos,” *Phys. Lett. B* **128**, 361 (1983).

[26] F. Bergsma *et al.* [CHARM Collaboration], “A Search for Decays of Heavy Neutrinos in the Mass Range 0.5-GeV

- to 2.8-GeV,” *Phys. Lett. B* **166**, 473 (1986).
- [27] D. S. Gorbunov and V. A. Rubakov, “Kaon physics with light sgoldstinos and parity conservation,” *Phys. Rev. D* **64**, 054008 (2001) [hep-ph/0012033].
- [28] S. V. Demidov and D. S. Gorbunov, “More about sgoldstino interpretation of HyperCP events,” *JETP Lett.* **84**, 479 (2007) [hep-ph/0610066].
- [29] M. Freytsis, Z. Ligeti and J. Thaler, “Constraining the Axion Portal with $B \rightarrow K l^+ l^-$,” *Phys. Rev. D* **81**, 034001 (2010) [arXiv:0911.5355 [hep-ph]].
- [30] P. Ball and R. Zwicky, “ $B(D,S) \rightarrow \rho, \omega, K^*, \phi$ decay form-factors from light-cone sum rules revisited,” *Phys. Rev. D* **71**, 014029 (2005) [hep-ph/0412079].
- [31] A. Pich, “Effective field theory: Course,” hep-ph/9806303.